Drug Design, Development and Therapy

Dovepress
open access to scientific and medical research

Open Access Full Text Article

ORIGINAL RESEARCH

Protective Effect of *Hedyotis diffusa* Willd. Ethanol Extract on Isoniazid-Induced Liver Injury in the Zebrafish Model

Xin Wang[1,2,*], Jie Zhao[1,2,*], Rui Zhang[1,*], Xinlu Liu[1], Chuanjiang Ma[2], Guangshang Cao[1,2], Yongli Wei[2], Peimin Yang[2]

[1]School of Pharmacy, Shandong University of Traditional Chinese Medicine (TCM), Jinan, 250355, People's Republic of China; [2]Grade Three Laboratory of TCM Preparation of National Administration of TCM, Affiliated Hospital of Shandong University of TCM, Jinan, 250014, People's Republic of China

*These authors contributed equally to this work

Correspondence: Peimin Yang, Tel +86-0531-68616607, Email jnypm@hotmail.com

Objective: This study aims to investigate the hepatoprotective effect and molecular mechanism of *Hedyotis diffusa* Willd. ethanol extract (HDWE) against isoniazid (INH)-induced liver injury in the zebrafish model.

Methods: INH-induced liver injury model was established by adding an immersion bath of INH in 3 days post-fertilisation (dpf) healthy transgenic zebrafish with liver-specific fluorescence (L-FABP: EGFP). HDWE and INH were given to the zebrafish to observe liver morphology and pathology, fluorescence intensity, and the activities of alanine aminotransferase (ALT), aspartate aminotransferase (AST) and superoxide dismutase (SOD), as well as the content of glutathione (GSH). The chemical composition of HDWE was analysed using high-performance liquid chromatography coupled with a quadrupole-time-of flight hybrid mass spectrometer (HPLC-Q-TOF-MS). The bioactive compounds, molecular targets and signalling pathways of HDWE were predicted using network pharmacology. Subsequently, molecular docking was adopted to analyze the affinities between the bioactive components and targets by Autodock. Finally, in vitro experiments were conducted to further verify the findings.

Results: Our findings showed that HDWE had a remarkable protective effect on INH-induced liver injury in zebrafish. Twenty compounds in HDWE were identified. Nineteen hub targets were identified as possible targets of HDWE, and a compound-target-pathway network was constructed. Nine bioactive compounds, ten molecular targets, and seven key signalling pathways were found to play a pivotal role in the hepatoprotective effect of HDWE against INH-induced liver injury. In vitro studies revealed that the important bioactive compound quercetin-3-O-sambubioside (QSA) could significantly reverse INH-induced cell viability decreases and had a significant effect on the associated targets predicted by network pharmacology and molecular docking.

Conclusion: In this study, through the research of hepatoprotective effect of HDWE and bioinformatics analysis, the bioactive compounds, important pathways and key molecular targets were discovered. These findings could provide scientific evidence for the use of HDW in liver injury and prove to help explore its efficacy and the mechanism of action.

Keywords: *Hedyotis diffusa* Willd., hepatoprotective activity, isoniazid-induced liver injury, zebrafish, network pharmacology, molecular docking

Introduction

Liver injury is an underlying cause of various liver diseases. Long-term liver injury can lead to fibrosis, cirrhosis, cancer, etc.[1] Drug-induced liver injury (DILI), also known as hepatotoxicity, refers to liver injury caused by the pharmaceutical compounds, dietary supplements and their metabolites.[2] DILI is the fifth leading cause of liver disease-related deaths globally.[3] In China, non-steroidal anti-inflammatory, antitubercular, antitumour, and drugs for metabolic diseases are the leading cause of DILI. Antitubercular drug-induced liver injury (ATB-ILI) is a predominant (21.99%) cause of DILI.[4]

Received: 17 January 2022
Accepted: 10 June 2022
Published: 27 June 2022

Isoniazid (INH), a first-line antitubercular drug, is reported to cause the highest incidence rate of liver injury (48%).[5] In general, biphenyl diester, bicyclic alcohol, tiopronin, reduced glutathione, polyene phosphocholine, adenosine methionine and vitamins are used to treat ATB-ILI. However, these drugs exhibit poor therapeutic effects and severe adverse reactions.[6] Thus, developing new therapy or drug to cure ATB-ILI is essential.

Traditional Chinese medicine (TCM) is reported to show greater benefits in improving patients' symptoms, protecting health, delaying disease progression and enhancing the body's ability to protect from liver injury.[7] The greater benefits of TCM are reported to be due to the presence of many compounds which act at various molecular targets and regulate multiple pathways.[8,9] *Hedyotis diffusa* Willd. (HDW) is a well-known traditional Chinese herbal medicine, and it is also a functional ingredient in teas and functional foods.[10] HDW is reported to possess anti-inflammatory, antioxidant, anticancer, and detoxification effects, and thus it has been used to treat various inflammatory diseases and cancers.[11–15] In the Chaoshan area of China, HDW is recognized as an excellent medication for liver protection, and it is also an essential component in Chinese patent medicines for treating liver illness, such as "Yiganning Keli", "Shuanghu Qinggan Keli" and "Ganfukang Wan". However, there is a little information on the possible hepatoprotective effect of HDW, bioactive compounds and molecular targets. Network pharmacology is an integrated analysis method in which the knowledge on the disease, target gene, target protein, and drug-drug interaction networks are integrated to predict the molecular targets. It has been widely used to predict the pharmacological mechanisms of TCM.[16–19] Thus, it can predict molecular targets, molecular pathways and bioactive compounds in HDW that are involved in its hepatoprotective effect.[20]

The tissues, organs and genetics of zebrafish are highly similar to those of humans. Thus, the zebrafish model is receiving increased attention in hepatoprotective screening.[21–23] In this study, we first evaluated the *Hedyotis diffusa* Willd. ethanol extract (HDWE) effect on INH-induced liver injury in the zebrafish model. High-performance liquid chromatography coupled with quadrupole time-of-flight mass spectrometry (HPLC-Q-TOF/MS) was used to identify the major compounds present in HDWE. The potential bioactive compounds, molecular targets and signalling pathways involved in hepatoprotective activity of HDWE were predicted using network pharmacology and molecular docking. Finally, the important findings were verified in vitro.The experiment protocol adopted in this study is shown in Figure 1.

Materials and Methods

Materials, Chemicals and Reagents

HDW is the dried whole grass of *Hedyotis diffusa* Willd. The HDW sample was purchased from Ji'an, Jiangxi Province (China), and authenticated by Professor Peimin Yang (Affiliated Hospital of Shandong University of TCM, Jinan, China). The voucher specimen (HDW-1-S10) was deposited in the Grade Three Laboratory of TCM Preparation of National Administration of TCM, Affiliated Hospital of Shandong University of TCM. INH was purchased from Fluka (Steinheim, Germany, purity higher than 99%, No. MKBQ8553V).

Quercetin-3-O-sambubioside (QSA) was obtained from Baoji Chenguang Biological Technology Co., Ltd. (Shanxi, China, purity higher than 98%, No. HS195101B2). HPLC-MS grade acetonitrile (Merck, Darmstadt, Germany), formic acid (Fluka, Steinheim, Germany), and ultrapure water (Huaren Yibao Drinks Co, Hong Kong, China) were used. Ethanol (analytical reagent, A.R.) was purchased from Sinopharm Chemical Reagent Co. Ltd. (Shanghai, China) and used for extraction. The zebrafish alanine aminotransferase (ALT) enzyme-linked immunosorbent assay (ELISA) kit, zebrafish aspartate aminotransferase (AST) ELISA kit, zebrafish superoxide dismutase (SOD) ELISA kit, zebrafish glutathione (GSH) ELISA kit and bicinchoninic acid (BCA) protein assay kit were purchased from Nanjing Jiancheng Bioengineering Institute (Nanjing, China, No.20200412, 20191215, 20190918, 20200318, 20200354). The human interleukin-6 (IL-6) and interleukin-2 (IL-2) ELISA kits were purchased from MultiSciences Biotech Co., Ltd. (Hangzhou, China, No.A10611124, A10211044). Hematoxylin-Eosin (HE) staining kit was purchased from Beijing Solaibao Technology Co., Ltd. (Beijing, China, No.20191218). Phosphate buffered saline (PBS), penicillin/streptomycin, dulbecco's modified eagle medium (DMEM) high glucose and tryptase were obtained from Biosharp Life Science (Shanghai, China). Fetal bovine serum (FBS) was purchased from Gibco company (New York, USA). Antibodies against PI3K p85, P-PI3K p85, AKT, P-AKT, NFKB p65, P-NFKB p65, Bcl-2 and GAPDH were purchased from Cell Signaling Technology (Boston, USA). All other reagents used were of analytical grade.

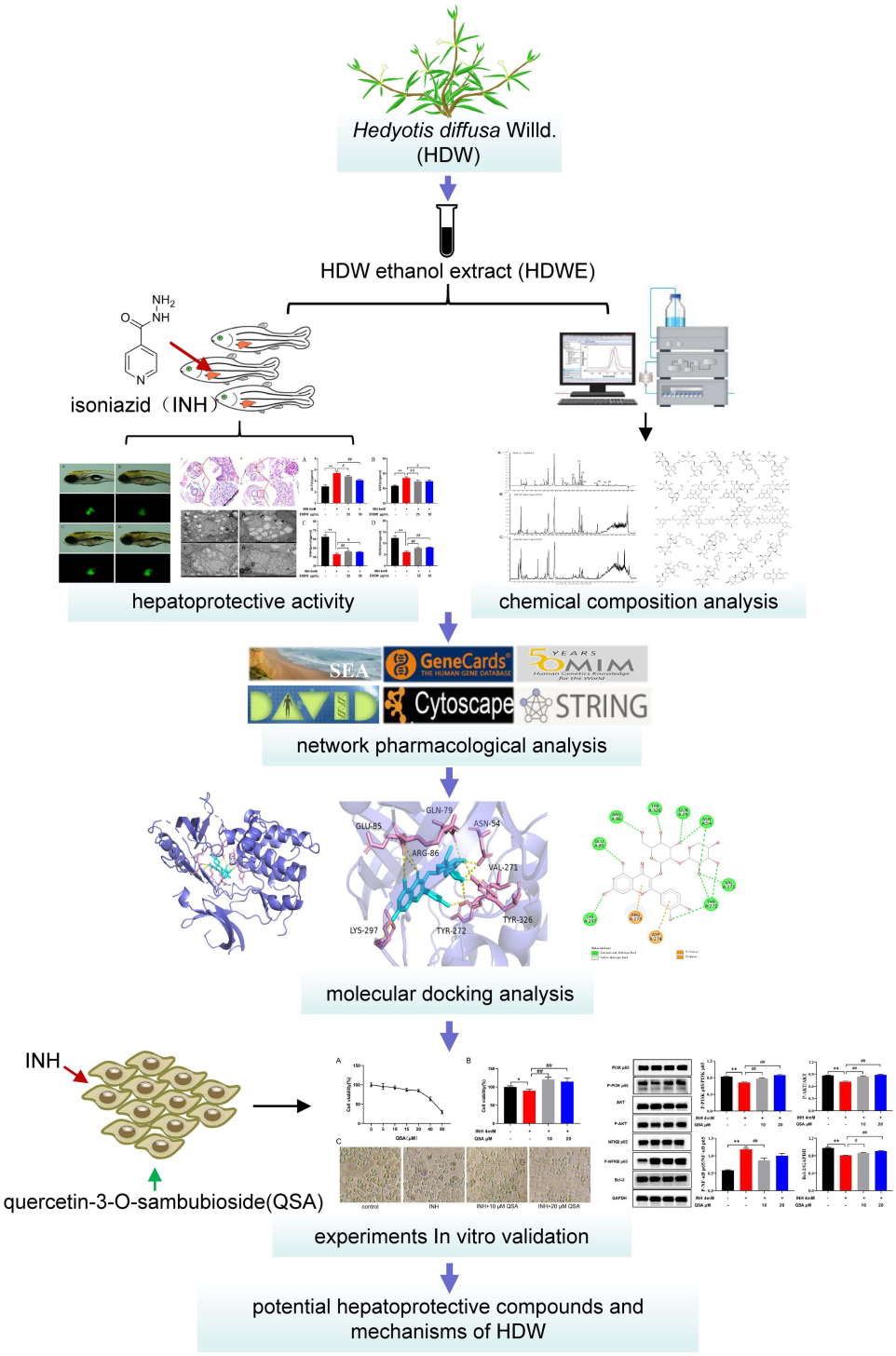

Figure 1 A framework for investigating the hepatoprotective effects of HDW in INH-induced liver injury in the zebrafish model and predicting the bioactive compounds molecular mechanisms.

Animals

The transgenic zebrafish with a liver-specific fluorescent probe (L-FABP: EGFP) were obtained from the Biology Institute, Qilu University of Technology (Jinan, China). They were maintained under standard conditions with alternating 14 h light/10 h dark cycles at 28 °C and fed twice daily with brine shrimp. Embryos were placed in zebrafish embryo culture water and incubated at 28 °C under controlled light for further analysis. All the experiments were carried out in

compliance with the standard ethical guidelines and approved by the Animal Ethics Committee of Affiliated Hospital of the Shandong University of TCM (Approval Number:2020114).

Preparation of HDWE

To obtain a homogeneous powder, the dried HDW was pulverised and sieved through a 10 mesh screen. Accurately weighed powder was extracted in an ultrasonic bath (power: 500 W, frequency: 40 kHz) with 15 volumes of 70% ethanol (v/v) at 60 °C for 45 minutes and filtered. The filtrate was concentrated under reduced pressure (temperature: 50~55 °C, pressure: −0.08~-0.1MPa) to obtain a concentrated solution whose relative density was 1.05~1.08 (temperature: 60 °C). The solution was allowed to flow through the SP825 macroporous adsorption resin column (column height/diameter: 7:1) at the rate of 6 times column volume (TCV)/h. The resin column was washed with 4 TCV and 30% ethanol-water (v/v). Then, the resin column was flushed with 10 TCV of 70% ethanol-water (v/v) at the rate of 7 TCV/h, and the solution was concentrated under reduced pressure (temperature: 50~55 °C, pressure: −0.08~-0.1 MPa) to a solution whose relative density was 1.10~1.15 (temperature: 60 °C). The concentrated solution was dried under reduced pressure (temperature: 50~60 °C, pressure: −0.08~-0.1 MPa) and powdered, used for further studies.

Experimental Procedures

The zebrafish embryos were developed for three days post fertilisation (dpf). The normal alive larvae were selected and placed in a 6-well plate (30 zebrafish larvae/well). The INH solution (4 mM) was added to each well to induce liver injury.[21] The INH and HDWE were dissolved in zebrafish embryo culture water (5 mM NaCl, 0.17 mM KCl, 0.4 mM $CaCl_2$, and 0.16 mM $MgSO_4$) to prepare the required concentration. The control group received the embryo culture water, the model group received 4 mM INH, and test groups received 4 mM INH plus different HDWE concentrations (600, 300, 150, 75, 50 and 25 μg/mL). All the experiments were done in triplicate. All the plates were hatched in an incubator at 28 °C with constant temperature and steady light. The compounds were added once a day for three days, and the culture medium was changed every day.

Assessment of Hepatoprotective Activity

Effect of HDWE on Zebrafish Survival

The survival and aberration rates of zebrafish larvae were used to evaluate the effect of HDWE on zebrafish. Cardiac arrest was used as the criterion for zebrafish death, and the aberration scores were determined by observing the general morphological features described by Panzica-Kelly.[24] The HDWE concentrations which were not toxic were used in the subsequent studies.

Microscopic Examination

Ten zebrafish larvae were randomly selected from each group, and the two-dimensional (2D) liver morphology of zebrafish was observed under a fluorescence microscope (Olympus SZX16; Tokyo, Japan). The fluorescence area and fluorescence intensity were measured using Image J software.

Pathological Examination

The zebrafish larvae were randomly selected and fixed with 4% paraformaldehyde and 2.5% glutaraldehyde. The larvae fixed with 4% paraformaldehyde were dehydrated with graded ethanol, then added xylene and embedded in paraffin. Then, Paraffin blocks were sectioned, stained with HE and mounted. Tissue sections were observed and photographed using a microscope (Olympus FSX100, Tokyo, Japan).

The zebrafish fixed with 2.5% glutaraldehyde were further fixed with 1% osmium acid, dehydrated using graded acetone and embedded in the embedding fluid. The embedding fluids were solidified, ultrathin sectioned, stained with uranium acetate, lead citrate, and mounted. Tissue sections were observed and photographed using a transmission electron microscope (TEM, Hitachi HT7800, Tokyo, Japan).

Detection of Liver-Related Enzyme Activities in Zebrafish

The tissue homogenate supernatant of 150 zebrafish was collected, and the BCA protein assay kit was applied to measure protein concentration of the collected supernatant. The activities of ALT, AST, and SOD, as well as the content of GSH, were determined and analysed according to the manufacturer's instructions.

HPLC-Q-TOF-MS Analysis of HDWE

Chromatographic peaks of the HDWE sample were identified and confirmed using a 6520 Accurate-Mass Q-TOF LC/MS instrument (Agilent, Santa Clara, USA). The chromatographic conditions for HPLC-ESI-Q/TOF-MS analysis were identical to our previous method.[10]

Network Pharmacology Study

Screening the Targets Acted by the Identified Constituents of HDWE

All constituents identified in the chemical profile of HDWE by HPLC-Q-TOF-MS were used to predict the potential action targets. We searched them from two databases: Swiss Target Prediction (http://www.swisstargetprediction.ch/) and Similarity ensemble approach (http://sea.bkslab.org/).[25,26] All the results were limited to "Homo sapiens", and the confidence score threshold was set as 0.8, with the targets selected after redundancy deletion.

Screening the Targets Related to Liver Injury

By searching with the terms "liver injury" and "Homo sapiens", genes related to liver injury were obtained from the databases of Genecards (http://www.genecards.org) and OMIM (Online Mendelian Inheritance in Man; http://www.omim.org/) after deleting redundancy of gene targets.[27]

Constructing the Protein-Protein Interaction(PPI) Network

The overlapping targets between the predicted targets of HDWE and the liver injury-related targets were chosen as the potential targets. Next, the potential targets were imported to the STRING (Search Tool for the Retrieval of Interacting Genes/Proteins) database (http://string-db.org/), only the targets with a higher fit score were higher than 0.9 were picked out. Based on the analysis of the STRING, we performed a topological analysis of the Cytoscape software (version 3.5.0, Boston, MA, USA)) in the interaction network according to the three parameters "Degree", "Betweenness Centrality" and "Closeness Centrality", and selected the median of the three parameters like the threshold.[28] After the second screening, the hub targets were obtained, and a PPI network of the significant targets was constructed, followed by visualisation using Cytoscape.

Gene Ontology Term Performance and Pathway Enrichment Analysis

Gene Ontology (GO) term performance and pathway enrichment analysis were conducted on the hub targets in the PPI network using the Kyoto Encyclopedia of Genes and Genomes(KEGG) (http://www.kegg.jp/) data obtained from the Database for Annotation, Visualization and Integrated Discovery (DAVID) platform (https://david.ncifcrf.gov/).[29,30] The *P*-values were calculated in these two enrichment analyses, and specific disease pathways were excluded. The value of $P<0.05$ suggests that the enrichment degree was statistically significant.

Construction of the Component-Target-Pathway Network

The integrated network of component-target-pathway was constructed using Cytoscape to identify the relationships of protein targets with each compound and the involved pathways, followed performed a topological analysis as described in 2.7.3 to screen the vital potential components, target, and pathways.

Molecular Docking

Through the above-network pharmacology analysis, the main active components and important key targets/signalling pathways in hepatoprotective activity of HDWE were obtained. The binding activities were verified by molecular docking to illustrate the relationship between the main active components and the key targets. Protein Data Bank (PDB) (http://www.rcsb.org) was used to obtain the X-ray crystal structures of the targets,[31] including AKT1 (PDB

ID:3O96), EGFR (PDB ID:6WXN), HRAS (PDB ID:2RGE), IL2 (PDB ID:1PW6), IL6 (PDB ID:2IL6), MAPK3 (PDB ID:2ZOQ), NFKB1 (PDB ID:1MDI), PIK3R1 (PDB ID:3I5S), RELA (PDB ID:2RAM) and SRC (PDB ID:4MXO). PyMOL 2.5 (https://pymol.org/2/) was then used to eliminate water molecules and pro-ligand small molecules.[32] The protein receptor files and ligand files were processed, and then converted to pdbqt format using AutoDock Tools 1.5.6. Each grid box was centered on ligand. And then, Autodock Vina 1.2.0 was used to perform molecular docking calculations and their affinity.[33] The best affinity conformation was chosen as the final docking conformation. By using PyMOL 2.5, the docking experiments were visualized and presented as 3D diagrams and 2D diagrams.

Experiments in vitro Validation

Cell Culture

L02 cells were purchased from Shanghai Institute of Biochemistry and Cell Biology (Shanghai, China). The cells were cultured in the DMEM with 10% FBS at 37°C in 5% CO_2 incubator.

Cell Counting Kit-8 (CCK-8) Assay

L02 cells were plated at the density of 1×10^5 cells/well into 96-well plates and cultured in DMEM with 10% FBS, treated with different concentration of QSA for 24 h. QSA of two concentrations (10μM, 20μM) were added to the cells 1h before INH treatment. Cell proliferation was measured by CCK-8 assay.

ELISA Assay

L02 cells were seeded in 6-well plates at 1×10^6 cells/well and incubated for 24h. The experiment was divided into four groups, including control group, INH group (INH: 4 mM), INH+QSA (L) group (INH: 4 mM, QSA:10 μM), INH+QSA (H) group (INH: 4 mM, QSA:20 μM). The culture supernatant was collected, the cells were lysed, and the protein content was determined. Finally, the levels of IL-6 and IL-2 were detected through corresponding ELISA kits according to the manufacturer's instructions.

Western Blot Analysis

The protein samples were mixed with SDS buffer and boiled for denaturation. Then, the protein was separated and transferred to the PVDF membranes. After blocked with 5% skim milk for 1h, the membranes were incubated with corresponding primary antibodies overnight at 4 °C, and then washed with TBST 3 times, incubated with the HRP-conjugated secondary antibody for 1 h at room temperature. The protein bands were detected with electro-chemiluminescence (ECL) reagent, and scanned using a chemiluminescence digital imaging system. The protein bands were analyzed by Image J software.

Statistical Analysis

The experimental data are expressed as the mean±SD. The data normality were assessed by the Shapiro–Wilk test and QQ plots. Statistical differences were analysed using analysis of variance (ANOVA). $P<0.05$ was considered significant, and $P<0.01$ was considered highly significant. All data were analysed using GraphPad Prism version 8.0 (GraphPad Software Inc, CA, USA).

Results

Intervention Concentration of HDWE

The surviving and aberration rates of zebrafish in different HDWE concentration intervention groups are shown in Table 1. The concentrations of 25 μg/mL and 50 μg/mL were selected for subsequent experiments.

Effects of HDWE on Morphological and Fluorescence Intensity of Liver

Compared to the control group, the liver fluorescence area and fluorescence intensity were significantly lower in model group, and compared with those in model group, the liver fluorescence area and fluorescence intensity were significantly higher in HDWE groups, as shown in Figure 2A and Table 2.

Table 1 Different Concentrations of HDWE on Zebrafish Embryonic Development

Description	Drug Concentration	Surviving Rate/%	Aberration Rate/%
Embryo culture water	—	100.0	0
INH+HDWE	4 mM+0 μg/m	98.0	9
	4 mM+600 μg/mL	0	—
	4 mM+300 μg/mL	12.5	100
	4 mM+150 μg/mL	16.7	60
	4 mM+75 μg/mL	98.0	22
	4 mM+50 μg/mL	100.0	14
	4 mM+25 μg/mL	100.0	10

Abbreviations: INH, isoniazid; HDWE, *Hedyotis diffusa* Willd. ethanol extract.

Effects of HDWE on the Pathological Changes in Liver Tissues

The results of HE staining showed that hepatocytes were significantly damaged in the model group compared with the control group. Hepatocytes in the model group had shown a sparse cytoplasm, nuclear atrophy, vacuolisation and aggregation of inflammatory cells. These phenotypes were improved in the HDWE group (Figure 2B).

On comparing the micrographs obtained from TEM (Figure 2C), the nucleus and all the mitochondria in the model group had distorted compared to the control group. Mitochondria showed variability in number, size, and shape, and the cristae membranes were seemed to be significantly reduced and disorganised. In the HDWE group, especially the 50 μg/mL HDWE group, the morphology of the nucleus and mitochondria has been significantly improved, and the cristae appeared denser was observed in mitochondria.

Effects of HDWE on ALT, AST, GSH and SOD Levels

Compared with those in the control group, the levels of the ALT, AST was significantly higher in the model group ($P<0.01$), but the GSH, SOD were significantly lower in the model group ($P<0.01$). Compared with the model group, the levels of ALT, AST was significantly lower in the HDWE group ($P<0.05$, or $P<0.01$), and the levels of GSH, SOD was significantly higher ($P<0.05$, or $P<0.01$), as shown in Figure 3.

Identification of Chemical Constituents of HDWE

The detection and identification of components of HDWE were conducted by HPLC-Q-TOF-MS (Figure 4). Altogether, twenty constituents, such as flavonoids and iridoids, were tentatively characterised by comparing with values reported by Ye et al.[34] The detailed information of all the components is listed in Table 3, and the structural information formulas are shown in Figure 5.

Putative Targets of HDWE

In total, 413 candidate targets involved in the therapeutic process of HDWE were selected from Swiss Target Prediction and Similarity ensemble approach databases. The detailed information is given in Supplementary Table S1.

Known Therapeutic Targets Acting on Liver Injury

Thirteen thousand one hundred eighty-one (13,181) known therapeutic targets associated with liver injury were screened from the Genecards database, and 246 known liver injury targets were derived from the OMIM database. After removing duplicate values, 12,907 targets related to liver injury were retained. The detailed information is given in Supplementary Table S2.

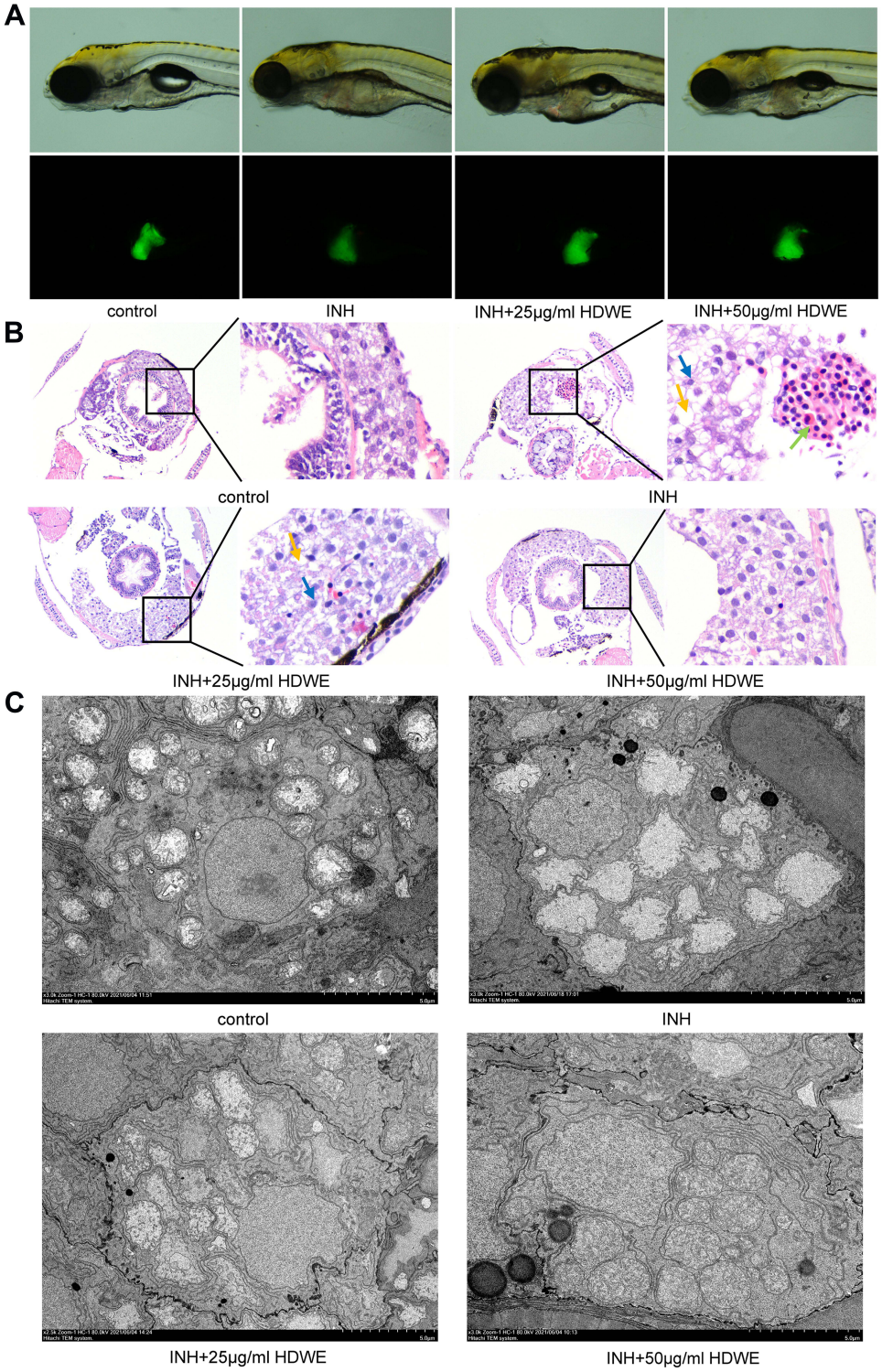

Figure 2 Effects of HDWE on morphological and pathological changes of liver. (**A**) Changes in morphology and fluorescence intensity. (**B**) Effects on liver tissue stained with HE. (**C**) Effects on liver tissue observed by TEM.
Notes: Yellow arrowheads indicate vacuole. Green arrowheads indicate the accumulation of inflammatory cells. Blue arrowheads indicate nuclear atrophy.
Abbreviations: INH, isoniazid; HDWE, *Hedyotis diffusa* Willd. ethanol extract.

PPI Network and the Significant Targets

A Venn diagram was established through Venny 2.1.0 (http://bioinfo.cnb.csic.es/tools/venny/index.html) to clarify the relationship between HDWE and liver injury-related targets, and the targets could be further intersected to obtain the

Table 2 Different Experimental Groups on Liver Fluorescence Area and Intensity

Experimental Groups	Drug Concentration	Fluorescence Area/ mm^2	Fluorescence Intensity/% of Control
Control group	—	34.21±1.33	100.0±18.04
Model group	4 mM INH	29.48±3.55*	48.30±10.64**
HDWE groups	4 mM INH+25 μg/mL HDWE	38.02±4.08##	59.31±11.45#
	4 mM INH+50 μg/mL HDWE	33.67±2.62#	67.25±12.64##

Notes: The data represent the mean ± SD (n=10). *P<0.05 vs control group; **P<0.01 vs control group; #P<0.05 vs model group; ##P< 0.01 vs model group.
Abbreviations: INH, isoniazid; HDWE, *Hedyotis diffusa* Willd. ethanol extract.

intersection (Figure 6). In Figure 6, the circle on the left represents HDWE putative targets, and on the right represents liver injury-related targets. Three hundred fifty-two (352) intersection targets were overlapping the two cycles, shown as the related targets of HDWE in treating the liver injury. The detailed information is given Supplementary Table S3.

To better understand the mechanism by which HDW protects the liver, a PPI network with 352 targets with a fit score higher than 0.9 was constructed (Figure 7A). Subsequently, all the nodes in the PPI network were analysed according to three topological parameters (degrees, betweenness centrality, and closeness centrality). Targets with values greater than the median were selected as hub targets to construct the core hub node of HDW for the treatment of liver injury

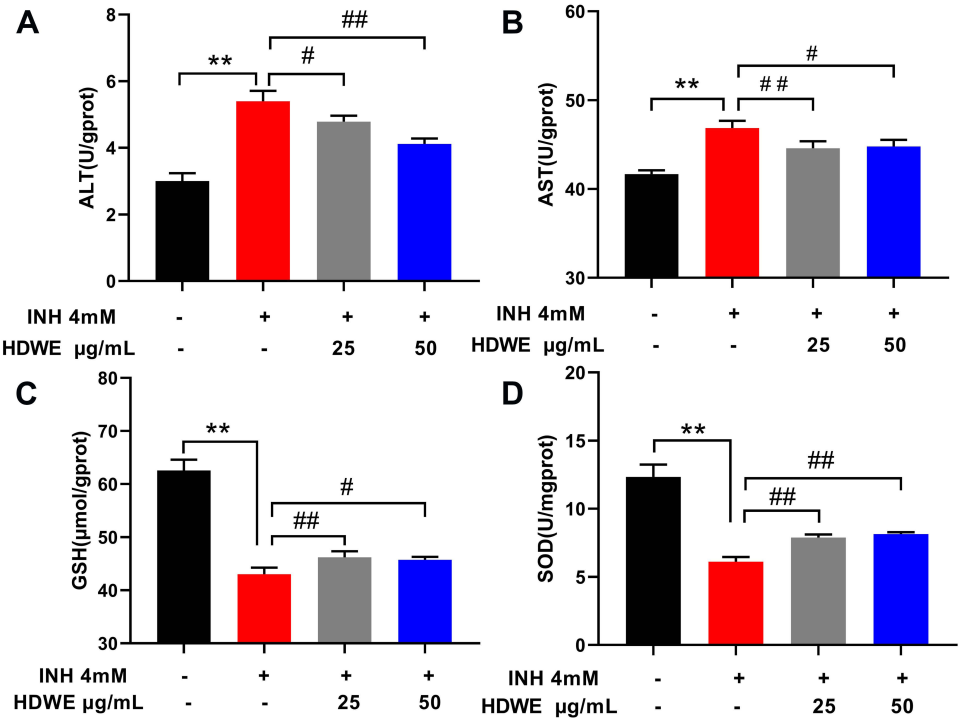

Figure 3 Effects of HDWE on ALT (**A**), AST (**B**), GSH (**C**) and SOD (**D**) levels. The data represent the mean ± SD (n=6). **P<0.01 vs control group; #P<0.05 vs model group; ##P< 0.01 vs model group.
Abbreviations: INH, isoniazid; HDWE, *Hedyotis diffusa* Willd. ethanol extract; ALT, the activities of alanine aminotransferase; AST, aspartate aminotransferase; SOD, superoxide dismutase; GSH, glutathione.

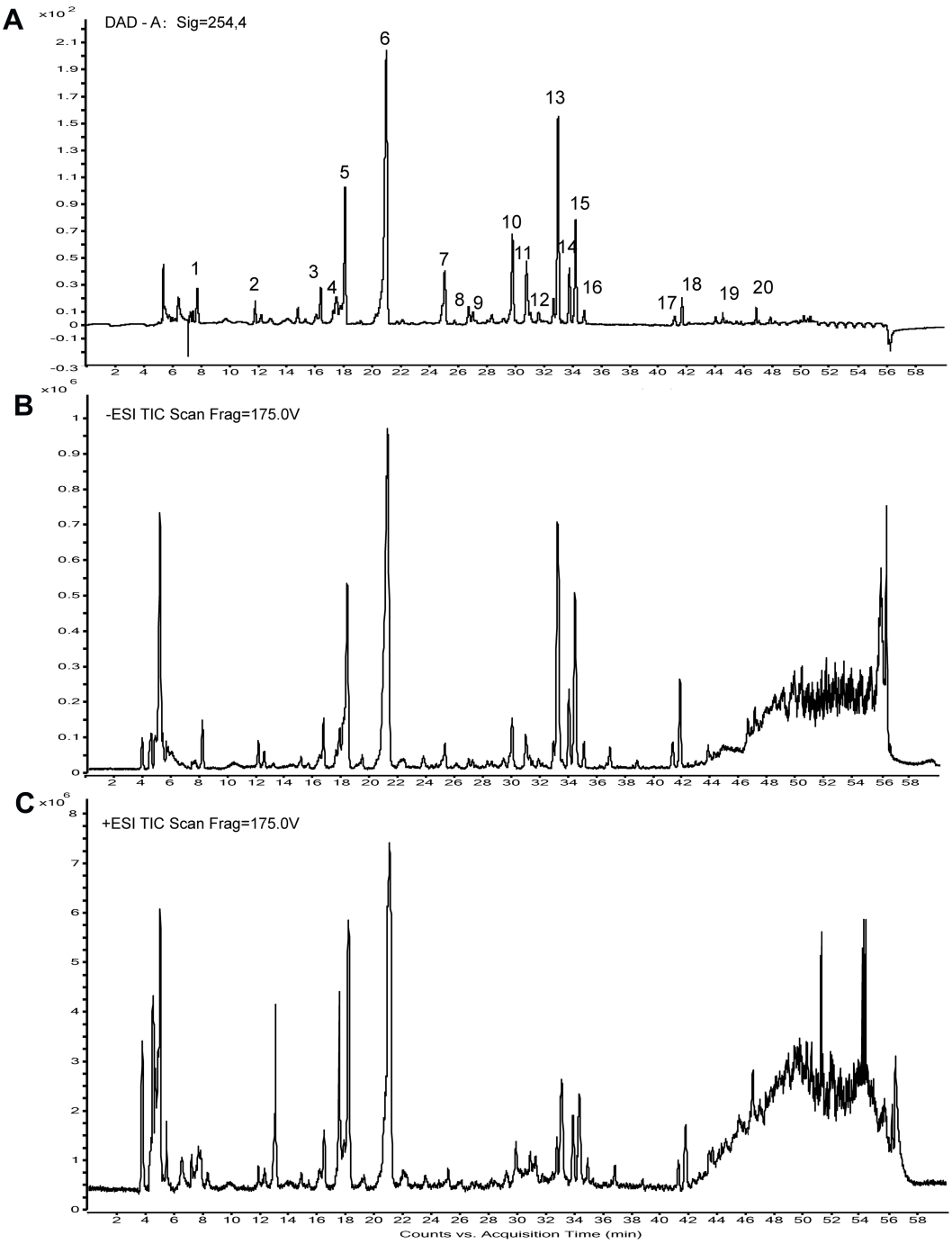

Figure 4 The HPLC chemical fingerprint and the total ion currents of HDWE.(**A**) The HPLC chemical fingerprint of HDWE. (**B**) The ion current of HDWE in negative ion mode. (**C**) The ion current of HDWE in positive ion mode.
Abbreviations: DAD, diode array detection; ESI, electrospray ionization; TIC, total ion current.

(Figure 7B). The 19 hub targets were PIK3R1, TNF, SRC, IL6, IL2, MAPK3, NFKB1, RELA, EGFR, HRAS, ESR1, APP, CXCL12, LCK, NR3C1, HSP90AA1, PTPN11, FOS, and PTK2.

GO Term Performance and Pathway Enrichment Analysis

GO enrichment analysis was carried out on the hub targets, and the top 10 GO terms ($P< 0.05$) were considered significant (Figure 8A–C). Most of these hub targets were enriched in the biological processes (BP), 1) transcription from

Table 3 HPLC-Q-TOF-MS Data of the Major Constituents of HDWE

Peak No.	tR (min)	Formula	Mass Ion (m/z)	Proposed Compound
1	7.89	$C_{16}H_{22}O_{11}$	389.1157 $[M- H]^-$, 413.1045 $[M+Na]^+$	Deacetylasperulosidic acid
2	11.91	$C_{16}H_{22}O_{11}$	389.1125 $[M- H]^-$, 413.1051 $[M+Na]^+$	Scandoside
3	16.19	$C_{17}H_{24}O_{11}$	427.1207 $[M+Na]^+$	Scandoside methyl ester
4	17.57	$C_{16}H_{22}O_8$	341.0849 [M- H]-	Coniferin
5	17.88	$C_{18}H_{24}O_{12}$	431.1173 $[M- H]^-$, 455.1166 $[M+Na]^+$	Asperulosidic acid
6	21.02	$C_{18}H_{22}O_{11}$	459.1068$[M+FA-H]^-$, 437.1013 $[M+Na]^+$	Asperulosidic
7	25.15	$C_{27}H_{30}O_{17}$	625.1287$[M- H]^-$, 649.1361$[M+Na]^+$	Quercetin-3-O-sophoroside
8	26.87	$C_{26}H_{28}O_{16}$	595.1759 $[M- H]^-$, 619.1261$[M+Na]^+$	Quercetin-3-O-sambubioside
9	27.15	$C_{21}H_{20}O_{12}$	609.1400$[M-H]^-$, 633.1411$[M+Na]^+$	Kaempferol-3-O-(2-O-β-D-glucopyranosyl)-β-D-galactopyranoside or isomer
10	29.93	$C_{38}H_{40}O_{21}$	831.1687 $[M- H]^-$, 855.1944 $[M+Na]^+$	Quercetin-3-O-[2-O-(6-O-E-sinapoyl)-β-D-glucopyranosyl]-β-D-galactopyranoside
11	30.91	$C_{37}H_{38}O_{20}$	801.1725 $[M- H]^-$, 825.1866 $[M+Na]^+$	Quercetin-3-O-[2-O-(6-O-E-feruloyl)-β-D-glucopyranosyl]-β-D-galactopyranoside
12	32.78	$C_{33}H_{38}O_{22}$	785.1979 $[M- H]^-$, 809.1921 $[M+Na]^+$	Kaempferol-3-O-[2-O-(6-O-E-feruloyl)-β-D-glucopyranosyl]-β-D-galactopyranoside
13/15	33.07/34.33	$C_{26}H_{30}O_{13}$	549.1514 $[M- H]^-$, 573.1582 $[M+Na]^+$	(E/Z)-6-O-(p-coumaroyl)scandoside methyl ester
14/16	33.89/34.92	$C_{27}H_{32}O_{14}$	579.1589 $[M- H]^-$, 603.1702$[M+Na]^+$	(E/Z)-6-O-(p-feruloyl)scandoside methyl ester
17/18	41.27/41.77	$C_{27}H_{32}O_{13}$	587.1728$[M+Na]^+$	(E/Z)-6-O-p-Methoxycinnamoyl scandoside methyl ester
19	46.44	$C_{30}H_{48}O_3$	457.3588$[M+H]^+$	Ursolic acid
20	47.18	$C_{16}H_{12}O_4$	267.0614 $[M- H]^-$, 269.0608 $[M+H]^+$	1-Hydroxy-2-methoxy-3-methyl-anthraquinone

Abbreviation: tR, retention time.

RNA polymerase II promoter, 2) epidermal growth factor receptor signalling, 3) ERK1 and ERK2 cascade, 4) ERBB2 signalling, 5) platelet activation, 6) nitric oxide biosynthetic process, 7) apoptotic process, 8) DNA-templated transcription, 9) Fc-epsilon receptor signalling and 10) phosphatidylinositol 3-kinase signalling. The hub targets were classified based on the molecular functions (MF), 1) identical protein binding, 2) protein tyrosine kinase activity, 3) nitric-oxide synthase regulator activity, 4) phosphatidylinositol-4,5-bisphosphate 3-kinase activity, 5) protein phosphatase binding, 6) transcription factor binding, 7) SH2 domain binding, 8) insulin receptor binding, 9) chromatin binding and 10) non-membrane spanning protein tyrosine kinase activity. Furthermore, most of the target responses were situated in various cellular components (CC), 1) cytosol, 2) cytoplasm, 3) membrane raft, 4) nucleus, 5) extracellular space, 6) perinuclear region of cytoplasm, and 9) plasma membrane.

KEGG pathway enrichment analysis was carried out to deduce the potential pathways, and in total, 82 valuable signal pathways ($P<0.05$) were identified. Subsequently, 20 significant pathways are presented in Figure 8D, 1) PI3K-AKT signalling pathway, 2) T cell receptor signalling pathway, 3) Chemokine signalling pathway, 4) VEGF signalling pathway, 5) Ras signalling pathway, 6) Toll-like receptor signalling pathway, 7) TNF signalling pathway, 8)

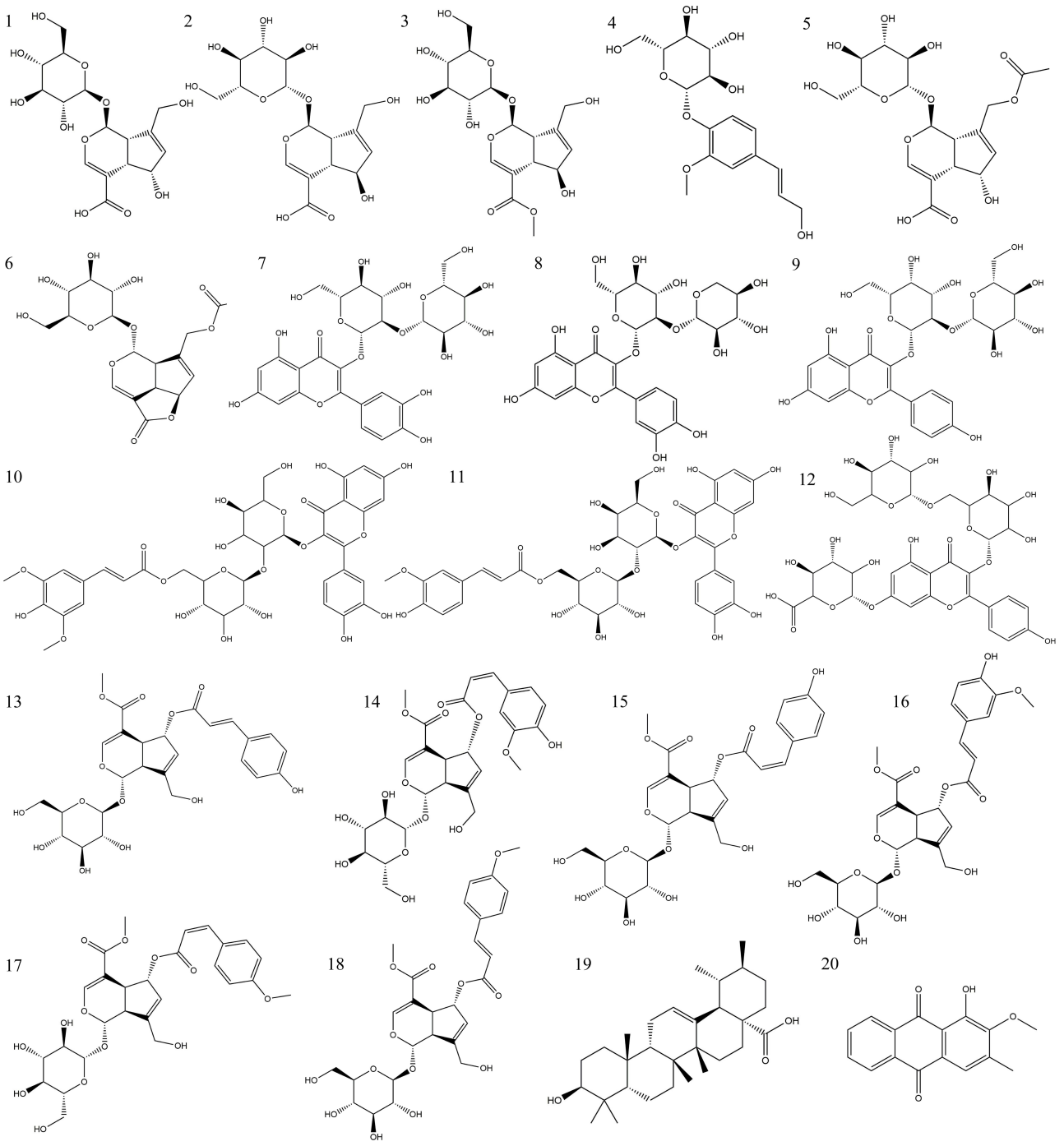

Figure 5 Chemical structures of the identified compounds from HDWE.

Sphingolipid signalling pathway, 9) NOD-like receptor signalling pathway, 10) MAPK signalling pathway, 11) Jak-STAT signalling pathway, 12) mTOR signalling pathway, 13) NF-kappa B signalling pathway, etc. These findings suggest that HDWE treatment of a liver injury may result from a complex of multiple pathways with synergistic effects.

Compound-Target-Pathway Network Analysis

To further investigate the connections between the HDWE bioactive ingredients, the hub targets and signalling pathways, the compound-target-pathway network was constructed and illustrated in Figure 9. The topological analysis predicted nine

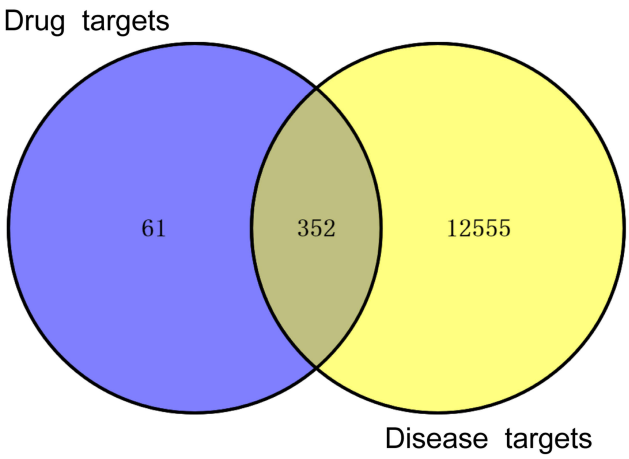

Figure 6 Intersection of HDWE targets and liver injury-related targets.

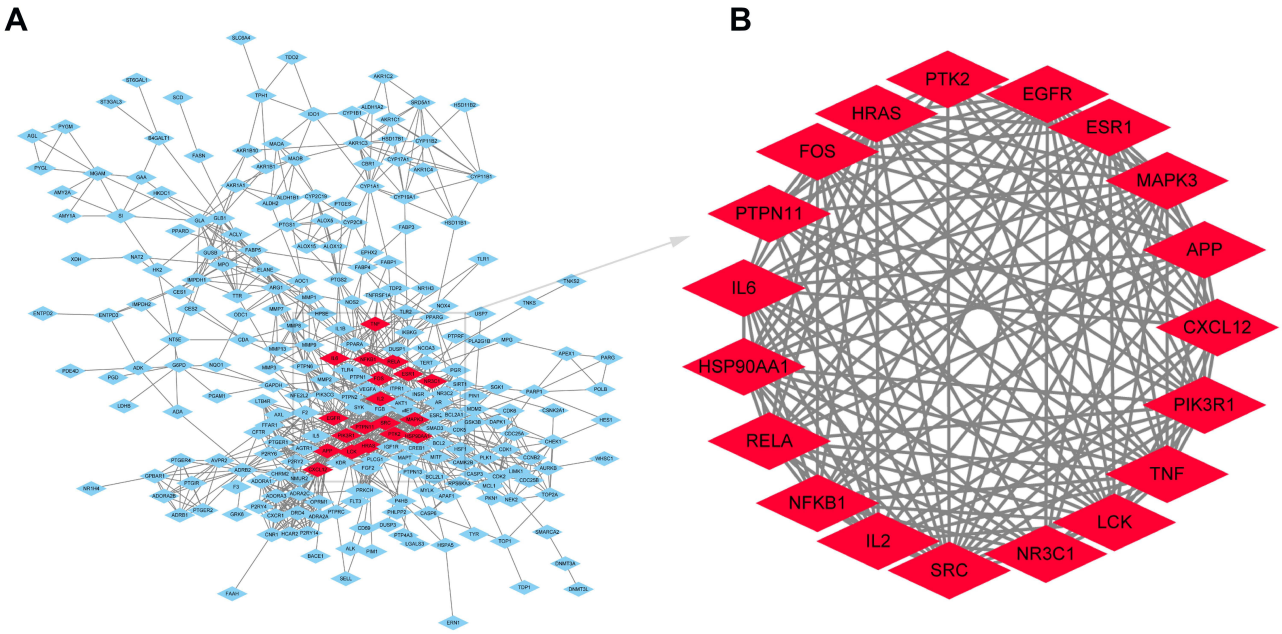

Figure 7 The PPI network and hub targets of HDWE. (**A**) PPI network of the 352 potential targets. (**B**) The hub targets of HDWE against liver injury identified by topological analysis.

compounds, ten targets, and seven signalling pathways. The compounds which were critical to the target are 1) (E/Z)-6-O-(p-feruloyl)-scandoside methyl ester, 2) quercetin-3-O-sophoroside, 3) coniferin, 4) 1-Hydroxy-2-methoxy- 3-methyl-anthraquinone, 5) kaempferol-3-O-(2-O-β-D-glucopyrano-syl)-β-D-galactopyranoside, 6) the isomer of 5), 7) quercetin-3-O-[2-O-(6-O-E-sinapoyl)-β-D-glucopy-mosyl]-β-D-glucopyranoside and 8) quercetin-3-O-sambubioside. The targets are 1) PIK3R1, 2) SRC, 3) IL6, 4) IL2, 5) MAPK3, 6) NFKB1, 7) RELA, 8) EGFR, 9) HRAS, and 10) AKT1. The key signalling pathways involved are 1) PI3K-AKT signalling pathway, 2) Chemokine signalling pathway, 3) Estrogen signalling pathway, 4) HIF-1 signalling pathway, 5) Ras signalling pathway, 6) B cell receptor signalling pathway, and 7) T cell receptor signalling pathway. These high-degree nodes in the network had more compound-target-pathway interactions, likely to play a greater role in liver protection. The detailed information is given in Supplementary Table S4.

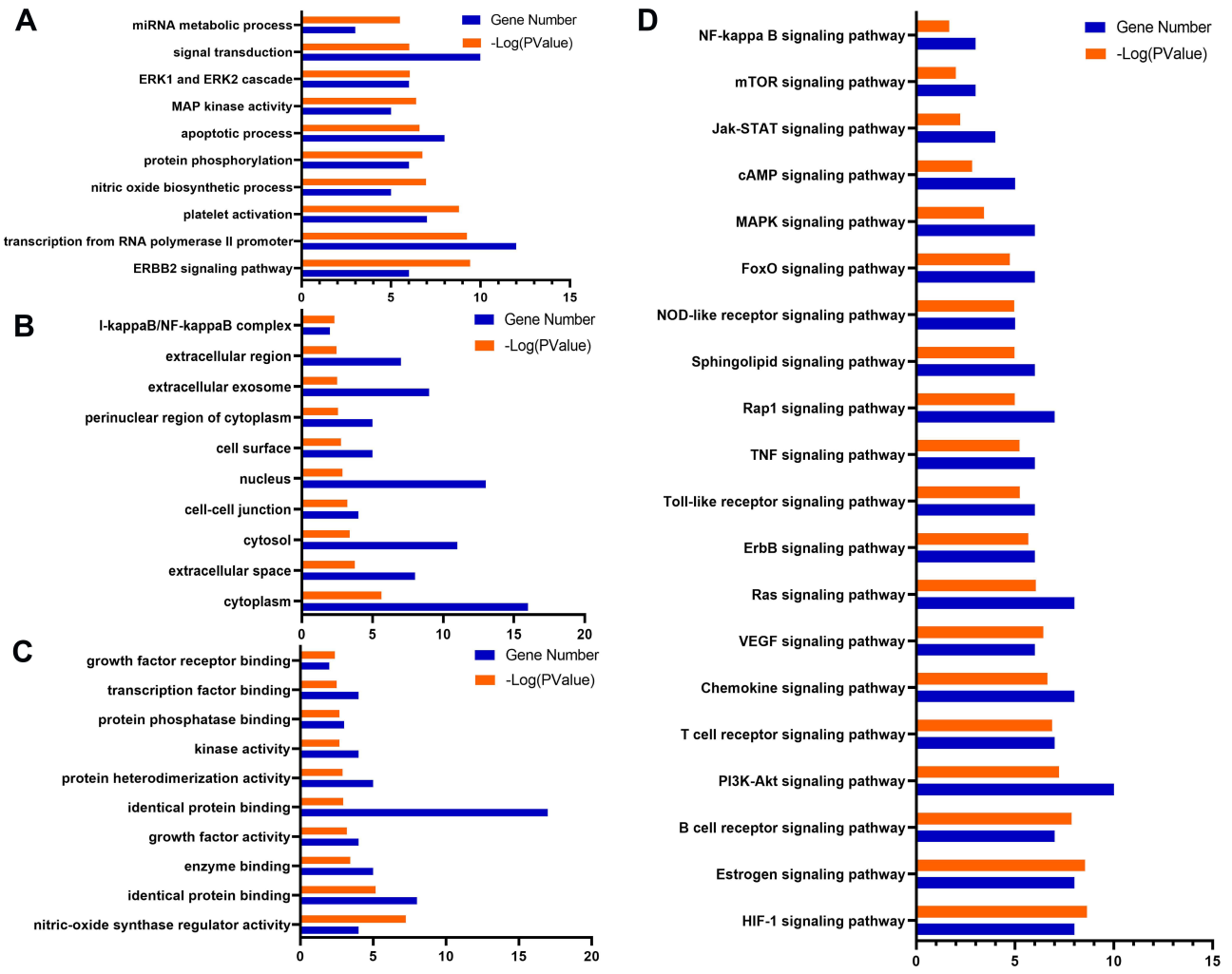

Figure 8 GO term performance and pathway enrichment analysis of hub targets related to liver injury. (**A**) GO enrichment analysis of hub targets for BP. (**B**) GO enrichment analysis of hub targets for CC. (**C**) GO enrichment analysis of hub targets for MF. (**D**) KEGG enrichment analysis of hub targets. The ordinate stands for GO terms or the main pathways, the primary abscissa stands for minus log 10(P), and the secondary abscissa stands for the number of major targets involved in the corresponding GO terms or the main pathways.

Molecular Docking Results

According to the above results, molecular docking was used to verify if the nine compounds had a significant role in regulating above ten targets. The binding energy was used to evaluate the activity between the docked molecules.The smaller the energy, the higher the affinity and the more stable the binding of the compound to the target site. The molecular docking results are shown in Figure 10, which shows that the binding energy of the nine compounds and ten targets were all less than −5.0 kcal/mol, indicating good binding activity.[34] Among them, the docking of AKT1 and QSA had the lowest binding energy (−10.0 kcal/mol), the docking of MAPK3 and QSA had the highest binding energy (−5.2 kcal/mol). QSA and AKT1 might be the most important compound and the most significant target.

Additionally, the bioactive components were successfully docked with the core targets, revealing a stable docking model with a specific binding site, binding distance, and binding atom. For example, QSA could bind to AKT1 by forming hydrogen bonds with the neighboring residues LYS-297, GLU-85, GLN-79, ARG-86, ASN-54, VAL-271, TYR-326 and pi interactions with ARG-273 and ASP-274 (Figure 11A). The stable point docking structure for the binding of the main components and targets were shown in Figure 11.

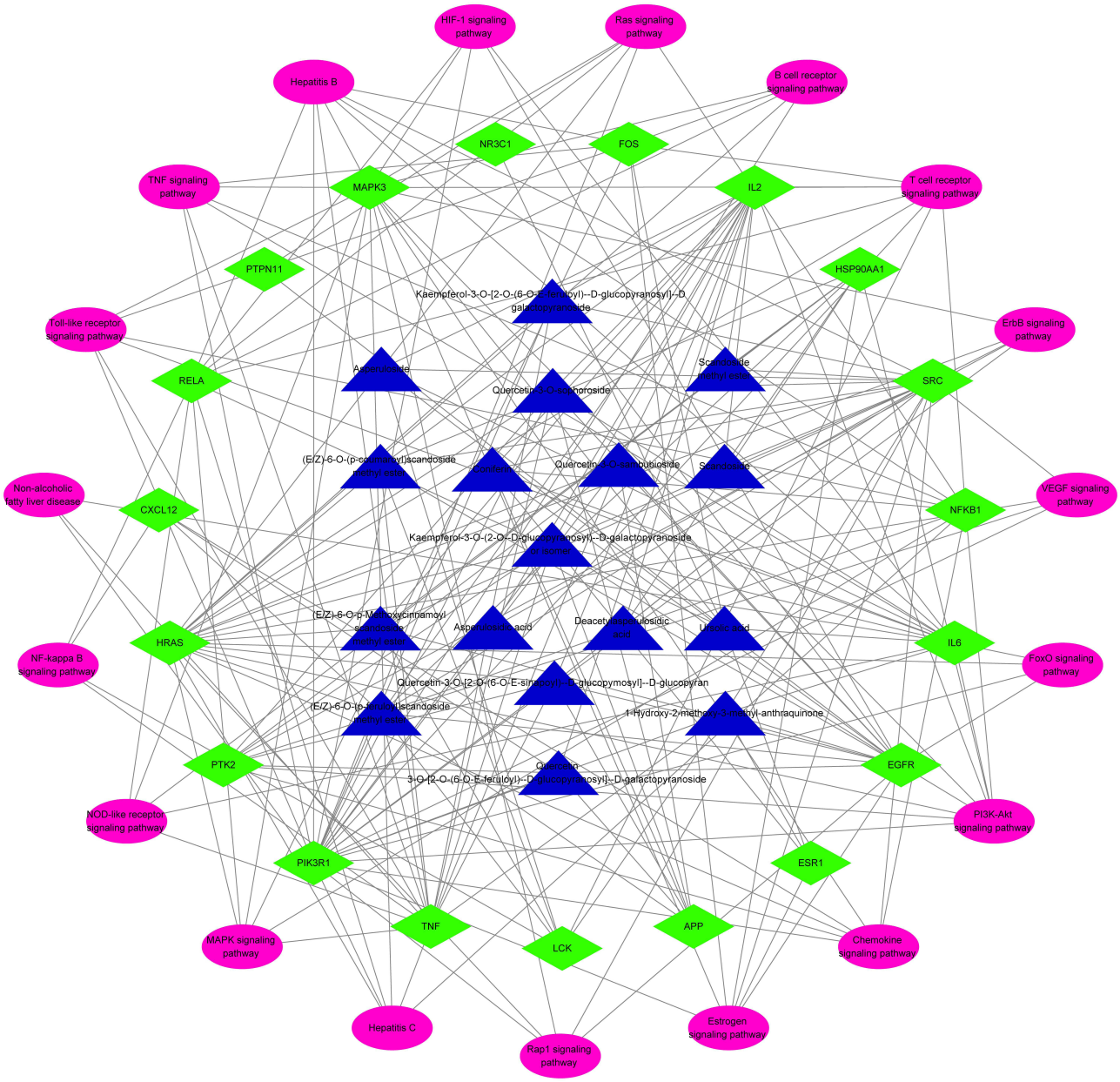

Figure 9 Network of compound-target-pathway against liver injury. Triangle nodes with blue denote bioactive of HDWE, rhombus nodes with green denote core targets of HDWE against liver injury, and oval nodes with pink denote the significant pathways.

Experiments in vitro Results

QSA as an important potential active component and the associated proteins (eg, PI3K p85, NFKB p65 and IL6, IL2, etc.) were determined for further experiment validation based on the network pharmacology and molecular docking results. We first detected the influence of different QSA concentrations on cell viability. According to the CCK8 assay result (Figure 12A), QSA of two concentrations (10 μM, 20 μM) were selected to test whether QSA protects L02 cells from INH-induced cytotoxicity. Importantly, from Figure 12B and C, we found that QSA (10 μM, 20 μM) obviously reversed INH-induced cell viability decrease and significantly improved the morphology of cells indicating a potential hepatoprotective effect.

As shown in Figure 13A and B, the levels of IL-6 and IL-2 in INH-induced L02 cells were significantly higher than those in the control group, whereas the levels of IL-6 and IL-2 in INH-induced L02 cells treated with QSA were

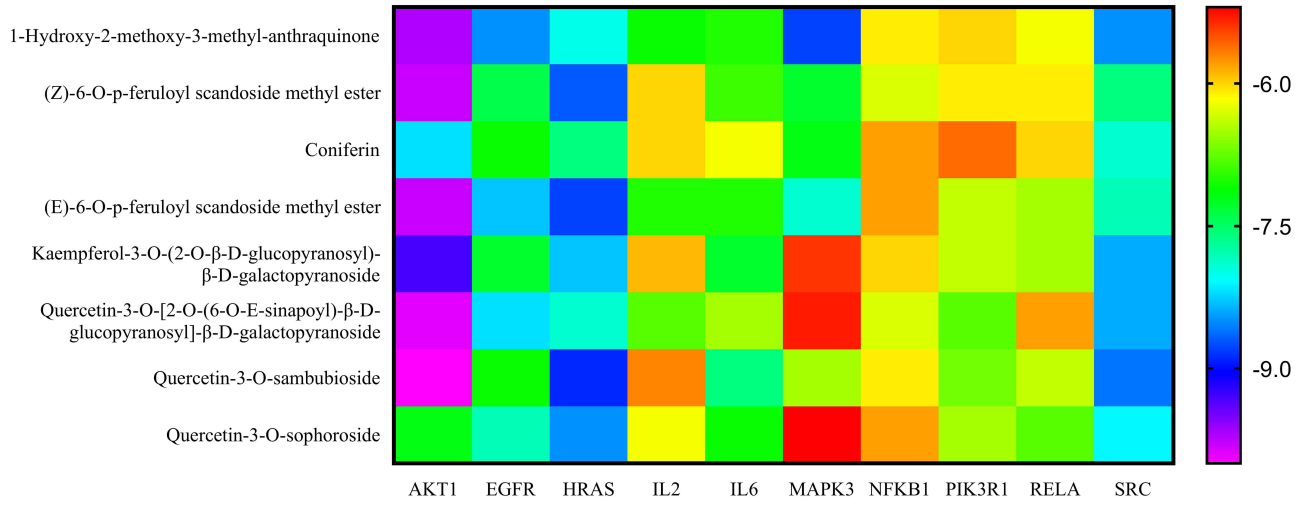

Figure 10 Binding energies (kcal/mol) of the nine compounds and ten targets via molecular docking.

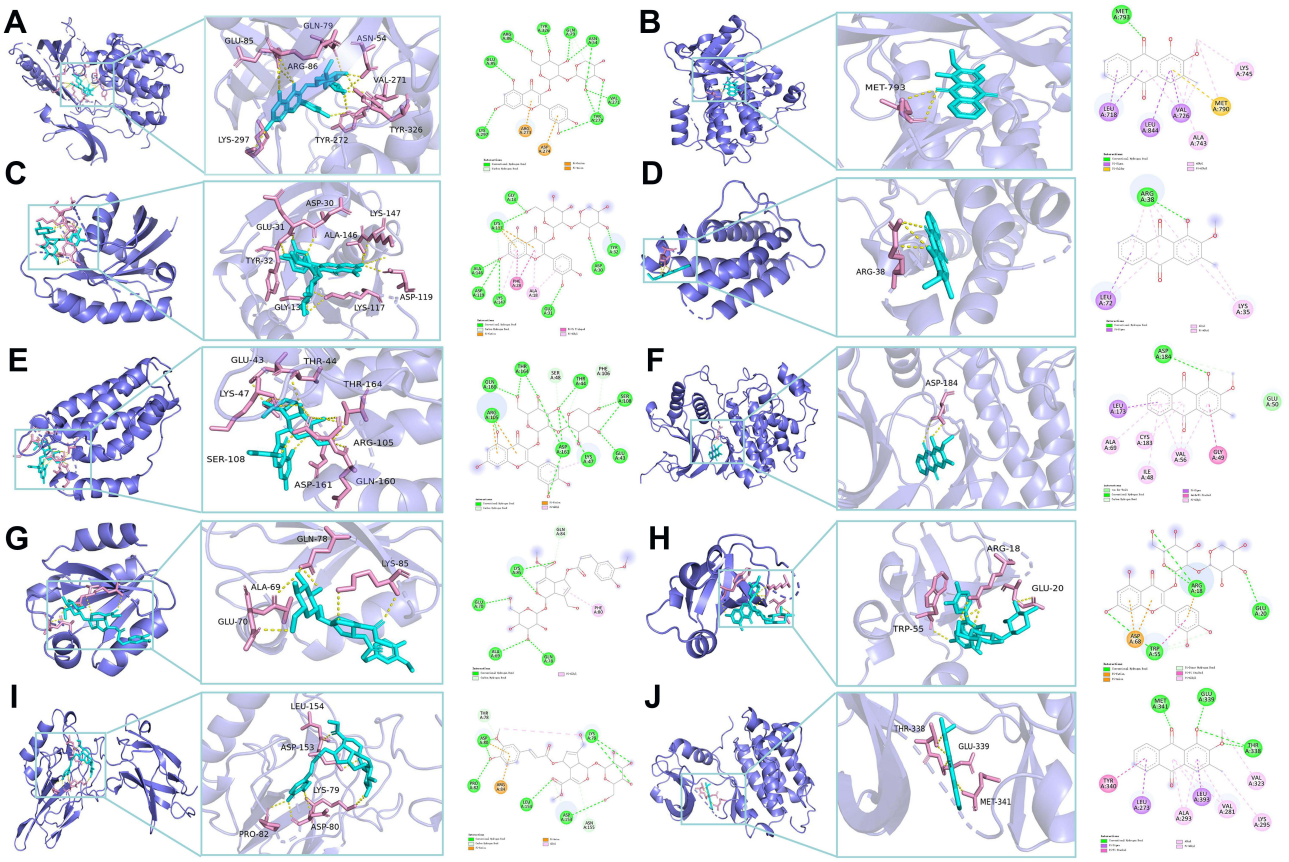

Figure 11 Molecular docking diagram of the ten targets and the main components. (**A**) AKT1/quercetin-3-O-sambubioside. (**B**) EGFR/1-Hydroxy-2-methoxy-3-methyl-anthraquinone. (**C**) HRAS/quercetin-3-O-sambubioside. (**D**) IL2/1-Hydroxy-2-methoxy-3-methyl-anthraquinone. (**E**) IL6/quercetin-3-O-sambubioside. (**F**) MAPK3/1-Hydroxy-2-methoxy-3-methyl-anthraquinone. (**G**) NFKB1/Z-6-O-p-feruloyl scandoside methyl ester.(**H**) PIK3R1/quercetin-3-O-sambubioside. (**I**) RELA/ E-6-O-p-feruloyl scandoside methyl ester. (**J**) SRC/quercetin-3-O-[2-O-(6-O-E-sinapoyl)-β-D-glucopyranosyl]-β-D-galactopyranoside.

significantly inhibited, of which the treatment effect of 20 μM QSA group was the best. The protein levels of PI3K p85, P-PI3K p85, AKT, P-AKT, NFKB p65, P-NFKB p65 and Bcl-2 in L02 cells were examined using Western blot analysis. Figure 13C–G indicated that the expression of P-PI3K p85, P-AKT and Bcl-2 was notably lower in the INH group

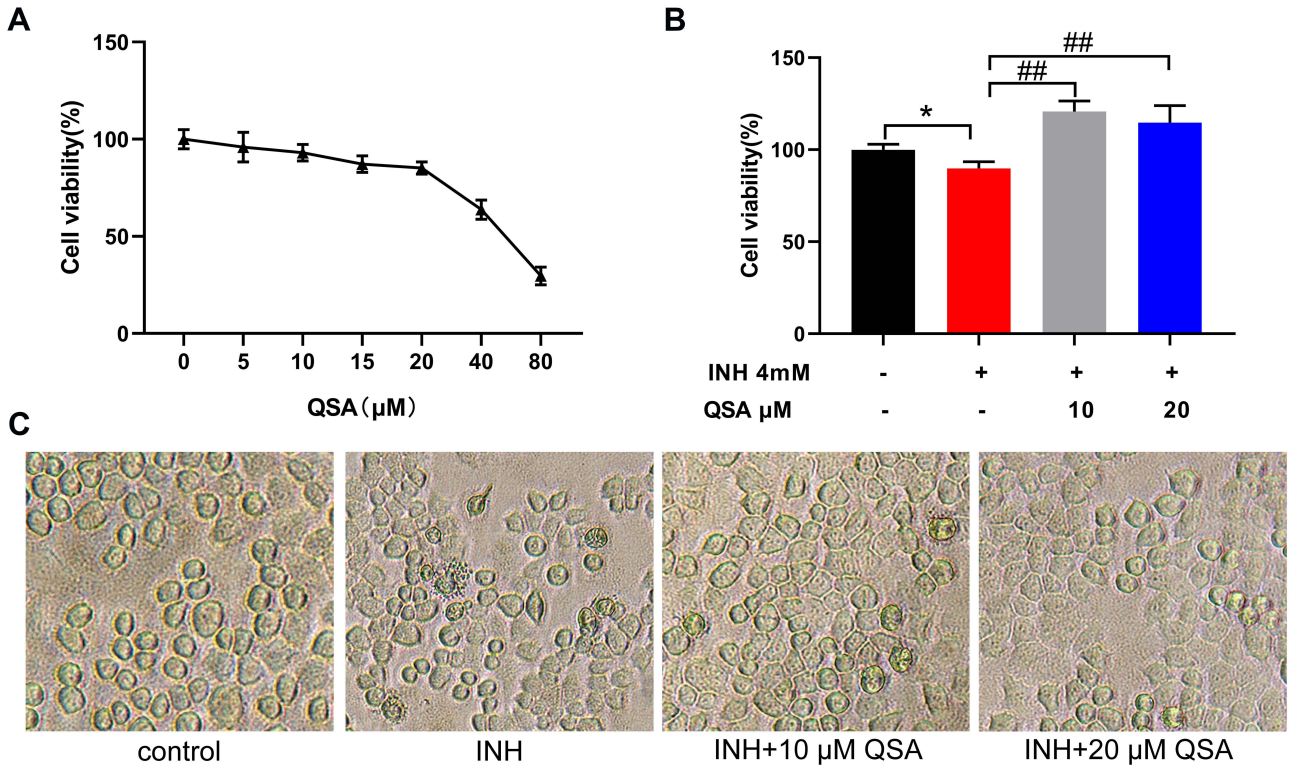

Figure 12 QSA reversed INH-caused the loss of cell survival rate in L02 cells. (**A**) Effects of different concentrations of QSA on cell survival rate of L02 cells. (**B**) QSA reversed INH-induced cell viability decrease. (**C**) Representative images of L02 cells morphology after QSA treatment. The data represent the mean ± SD (n=6). **P*<0.05 vs control group; ##*P*< 0.01 vs model group.
Abbreviations: INH, isoniazid; QSA, quercetin-3-O-sambubioside.

compared to the control group, but the expression of P-NFKB p65 was significantly higher. As compared to the INH group, the QSA group significantly increased the expression of P-PI3K p85, P-AKT, and Bcl-2, with L02 cells treated with 20 μM QSA having the best effect, while inhibiting the P-NFKB p65, with 10 μM QSA having the best effect. These findings indicate that QSA may play a hepatoprotective effect in INH-induced liver injury through the PI3K-AKT signalling pathway, which further validated the network pharmacology and molecular docking results that quercetin is an important component in HDW against INH-induced liver injury.

Discussion

Liver injury is an urgent problem and research hotspot in treating INH against tuberculosis, and new approaches or drugs for the therapy of INH-induced liver injury ought to be developed. HDW, traditional herbal medicine, and the active ingredients for tea and functional foods are excellent treatments for various inflammatory diseases and tumours. Still, its anti-liver injury effect was rarely reported. In the present study, we first investigated the effects of HDWE on INH-induced liver injury in zebrafish focused on the following aspects of morphological, fluorescence intensity, pathological examination of liver, and the activities of ALT, AST and SOD, as well as the content of GSH. Our experimental results illustrated that HDWE has a remarkable protective ability against INH-induced liver injury. TCM, such as glycyrrhizic acid preparations, may have protective effects on several DILI. As a response, in the future, we will explore the protective effects of HDWE on different DILI in order to expand the therapeutic applicability of HDWE.

The TEM micrographs revealed that HDWE could significantly improve the morphology of mitochondria, indicating that mitochondria may be an important target of HDWE in antagonising INH-induced liver injury. Similarly, some signalling pathways discovered in network pharmacology research are closely related to mitochondrial functions, such as the PI3K-AKT signalling pathway, which can regulate mitochondrial biosynthesis and energy metabolism,[35,36] the HIF-1

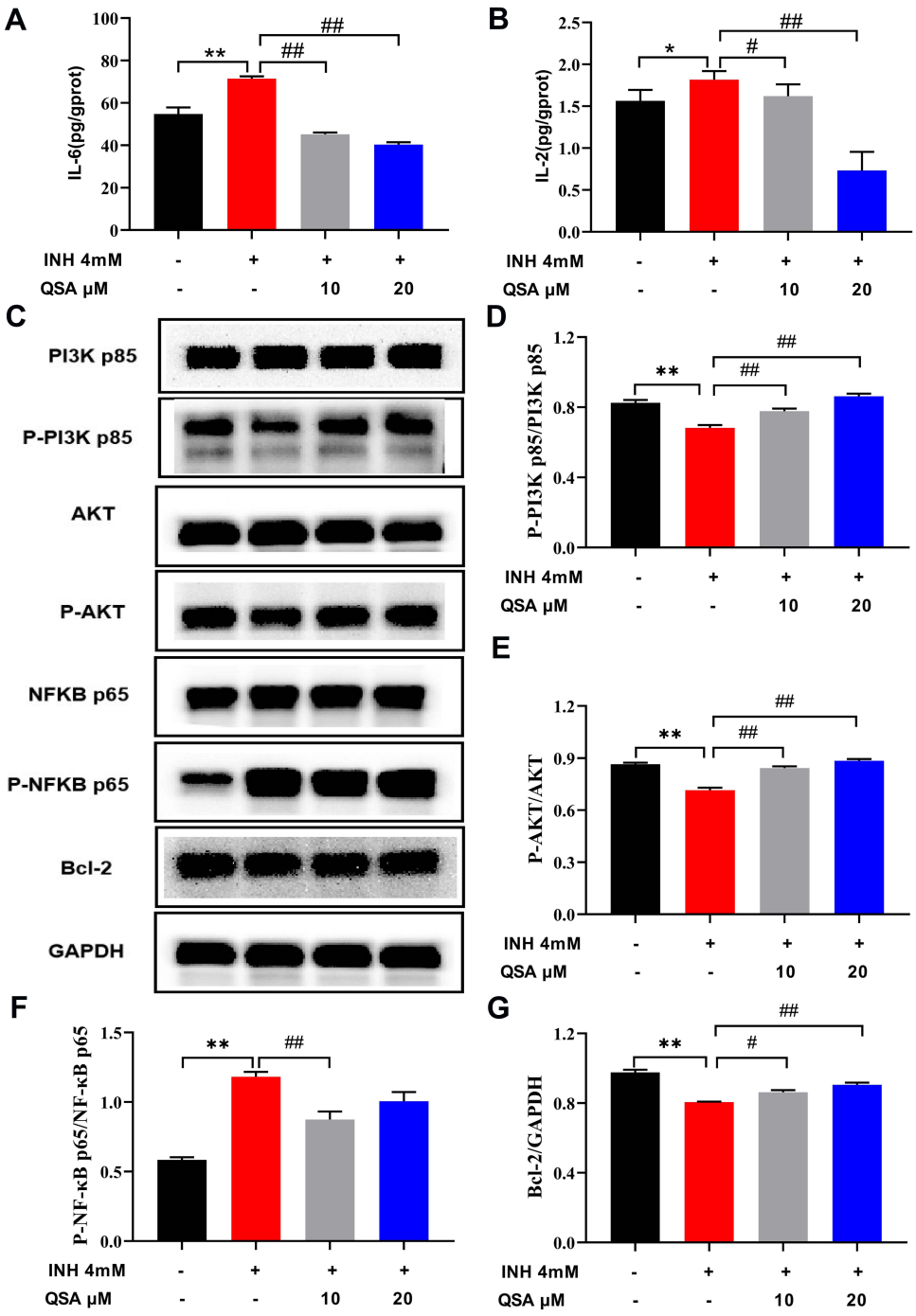

Figure 13 The effect of QSA on the associated proteins in INH-induced L02 cells. (**A**) Effects on the levels of IL-6. (**B**) Effects on the levels of IL-2. (**C**) Representative immunoblotting images of PI3K p85, p-PI3K p85, AKT, p-AKT, NFKB p65, p-NFKB p65, Bcl-2 and GAPDH. (**D**–**G**) Gray value statistics of corresponding proteins. The data represent the mean ± SD (n=3). *P<0.05 and **P<0.05 vs control group; #P< 0.05 and ##P< 0.01 vs model group.
Abbreviations: INH, isoniazid; QSA, quercetin-3-O-sambubioside.

signalling pathway, which can affect electron leakage in the mitochondrial electron transport chain,[37] and the Ras signalling pathway, which is related to the expression of key enzymes in the mitochondrial respiratory chain complex.[38,39] Consequently, we speculated that regulation of mitochondrial functions might be the possible mechanism underlying the action of the hepatoprotective potential of HDWE against INH-induced liver injury.

Network pharmacology analysis can identify the relationship between the compounds and targets/pathways. However, most network pharmacology studies collected herbal constituents from online databases to construct the compound-target

network. The screened bioactive compounds might be inconsistent with those existing in the herbal extract, which produced false-positive results. Therefore, in the subsequent work, the chemical constituents of HDWE were detected by our previous HPLC-ESI-Q/TOF-MS method. Twenty major compounds were identified; 1) eleven iridoids, 2) six flavonoids, 3) one phenylpropanoid, 4) one pentacyclic triterpene, and 5) one anthraquinone. Iridoids, such as deacetylasperulosidic acid, scandoside, scandoside methyl ester, asperulosidic acid, asperulosidic, are reported to 1) lower cholesterol levels, 2) protect the liver, 3) exhibit anti-inflammatory effect and 4) antitumour effect.[40,41] Flavonoids, such as quercetin-3-O-sophoroside, quercetin-3-O-sambubioside and quercetin-3-O-[2-O-(6-O-E-sinapoyl)-β-D-glucopyranosyl]-β-D-galactopyranoside, are reported to reduce blood cholesterol concentration, liver toxicity, liver damage, and liver fibres.[42–44] These reports provide supports and evidences for the reliability and accuracy of network pharmacology predicting hepatoprotective active ingredients in HDWE. However, we only conducted in vitro analysis of HDWE components, and an vivo study will be performed in the future to support and develop our research findings.

HDWE contains various active components that can antagonise liver injury through multiple targets, specific biological processes and related pathways. In this research, a total of 413 predicted targets of 20 HDWE components and 12,907 liver injury related targets were obtained. 352 HDWE-liver injury common targets were then screened and 19 hub targets were identified by topological analysis in the HDWE-liver injury common-targets network. After that, GO and KEGG pathway enrichment analyses were applied on the 19 hub targets. The GO functional enrichment analysis predicted that HDWE suppresses the liver injury by regulating 1) transcription from RNA polymerase II promoter, 2) epidermal growth factor receptor signalling, 3) ERK1 and ERK2 cascade, 4) ERBB2 signalling, 5) platelet activation, 6) nitric oxide biosynthetic process, 7) apoptotic process, 8) DNA-template transcription, 10) Fc-epsilon receptor signalling and 11) phosphatidylinositol 3-kinase signalling. KEGG pathway enrichment analysis indicated that the core targets related to liver injury could participate in 20 crucial signalling pathways. These include signalling pathways related to inflammation (TNF, MAPK, and NFKB); liver diseases (hepatitis B, hepatitis C, and non-alcoholic fatty liver disease); immunity (Toll-like receptor and NOD-like receptor); and angiogenesis (HIF-1 and VEGF). PI3K-AKT and FoxO signalling pathways are involved in cell proliferation, differentiation, apoptosis, and other signalling pathways related to cancer. Therefore, various compounds in HDWE might act on multiple targets and pathways. These compounds might play a pivotal role in preventing and treating liver injury, mainly through signalling pathways involving inflammation, immunity, cell proliferation and differentiation, and liver disease-related modules.

In addition, we developed a "compound-target-pathway" map based on the findings above. According to the topological analysis results, nine bioactive compounds, ten molecular targets, and seven key signalling pathways were found to play a pivotal role in the hepatoprotective effect of HDWE against INH-induced liver injury. Furthermore, molecular docking was conducted to analyse the binding activities between the nine bioactive compounds and the ten targets. The results showed that the nine bioactive compounds had good binding activities to the ten targets, and these compounds may be the active ingredients in HDWE that are involved in its hepatoprotective effect. AKT is considered to be a regulator of cell growth, survival, metabolism, and proliferation.[45] It has been demonstrated that AKT can be activated by PI3K and controls apoptosis by inhibiting NFKB activation.[46,47] According to in vitro validation results, QSA may be a key hepatoprotective component of HDWE, and the PI3K-AKT signaling pathway may play a role in its hepatoprotective action. However, since the validation was only a small sample (n=3) analysis, further studies with an expanded sample size need to be carried out to corroborate the findings.

Conclusion

Herbal medicines, featured as multiple herbs, ingredients and targets, have accumulated a great deal of valuable experience in preventing and treating the liver injury. However, the exact molecular mechanisms are still unclear. This study confirmed that HDW extract exerts liver-protective effects in an INH-induced liver injury zebrafish model. Moreover, we investigated the liver-protective constituents of HDW and the mechanism of action using the HPLC-ESI-Q/TOF-MS approach combined with network pharmacology analysis.

These findings could provide scientific evidence for the use of HDW in liver injury and prove to help explore its efficacy and the mechanism of action.

Acknowledgments

This work was financially supported by the National Natural Science Foundation of China (NSFC, Grant No. 82104506).

Disclosure

We declare that there is no conflict of interest regarding the publication of this paper.

References

1. Luedde T, Kaplowitz N, Schwabe RF. Cell death and cell death responses in liver disease: mechanisms and clinical relevance. *Gastroenterology*. 2014;147(4):765–783. doi:10.1053/j.gastro.2014.07.018
2. Andrade RJ, Chalasani N, Björnsson ES, et al. Drug-induced liver injury. *Nat Rev Dis Primers*. 2019;5(1):58. doi:10.1038/s41572-019-0105-0
3. Björnsson ES. Epidemiology, predisposing factors, and outcomes of drug-induced liver injury. *Clin Liver Dis*. 2020;24(1):1–10. doi:10.1016/j.cld.2019.08.002
4. Shen T, Liu Y, Shang J, et al. Incidence and etiology of drug-induced liver injury in Mainland China. *Gastroenterology*. 2019;156(8):2230–2241. doi:10.1053/j.gastro.2019.02.002
5. Hoofnagle JH, Björnsson ES. Drug-induced liver injury - types and phenotypes. *N Engl J Med*. 2019;381(3):264–273. doi:10.1056/NEJMra1816149
6. Norman BH. Drug Induced Liver Injury (Dili). Mechanisms and medicinal chemistry avoidance/mitigation strategies. *J Med Chem*. 2020;63(20):11397–11419. doi:10.1021/acs.jmedchem.0c00524
7. Xie J, Wang W, Dong C, et al. Protective effect of flavonoids from Cyclocarya paliurus leaves against carbon tetrachloride-induced acute liver injury in mice. *Food Chem Toxicol*. 2018;119:392–399. doi:10.1016/j.fct.2018.01.016
8. Gong JY, Ren H, Peng SY, et al. Comparative effectiveness of glycyrrhizic acid preparations aimed at preventing and treating anti-tuberculosis drug-induced liver injury: a network meta-analysis of 97 randomized controlled trials. *Phytomedicine*. 2022;98:153942. doi:10.1016/j.phymed.2022.153942
9. Hong M, Li S, Tan HY, Wang N, Tsao SW, Feng Y. Current status of herbal medicines in chronic liver disease therapy: the biological effects, molecular targets and future prospects. *Int J Mol Sci*. 2015;16(12):28705–28745. doi:10.3390/ijms161226126
10. Wang X, Ma CJ, Yang PM, et al. Integrated HPLC fingerprinting and multivariate analysis differentiates between wild and cultivated *Hedyotis diffusa* Willd. *Ind Crops Prod*. 2020;148:112223. doi:10.1016/j.indcrop.2020.112223
11. Wang X, Ma CJ, Yang PM, et al. Research progress of anti-inflammatory and anti-tumor effects of *Hedyotis diffusa* Willd. *Chin J Mod Appl Pharm*. 2020;37(19):2420–2427.
12. Zhang R, Ma C, Wei Y, et al. Isolation, purification, structural characteristics, pharmacological activities, and combined action of *Hedyotis diffusa* polysaccharides: a review. *Int J Biol Macromol*. 2021;183:119–131. doi:10.1016/j.ijbiomac.2021.04.139
13. Han X, Zhang X, Wang Q, Wang L, Yu S. Antitumor potential of *Hedyotis diffusa* Willd: a systematic review of bioactive constituents and underlying molecular mechanisms. *Biomed Pharmacother*. 2020;130:110735. doi:10.1016/j.biopha.2020.110735
14. Zhao L, Deng J, Xu ZJ, et al. Mitigation of aflatoxin B1 hepatoxicity by dietary *Hedyotis diffusa* is associated with activation of NRF2/ARE signaling in chicks. *Antioxidants*. 2021;10(6):878. doi:10.3390/antiox10060878
15. Li YL, Chen X, Niu SQ, Zhou HY, Li QS. Protective antioxidant effects of amentoflavone and total flavonoids from *Hedyotis diffusa* on H_2O_2 - induced HL-O2 cells through ASK1/p38 MAPK pathway. *Chem Biodivers*. 2020;17(7):e2000251. doi:10.1002/cbdv.202000251
16. Hopkins AL. Network pharmacology: the next paradigm in drug discovery. *Nat Chem Biol*. 2008;4(11):682–690. doi:10.1038/nchembio.118
17. Li S, Zhang B, Zhang N. Network target for screening synergistic drug combinations with application to traditional Chinese medicine. *BMC Syst Biol*. 2011;5:S10. doi:10.1186/1752-0509-5-S1-S10
18. Li X, Yang H, Xiao J, et al. Network pharmacology based investigation into the bioactive compounds and molecular mechanisms of Schisandrae Chinensis Fructus against drug-induced liver injury. *Bioorg Chem*. 2020;96:103553. doi:10.1016/j.bioorg.2019.103553
19. Tian D, Yang Y, Yu M, et al. Anti-inflammatory chemical constituents of Flos Chrysanthemi Indici determined by UPLC-MS/MS integrated with network pharmacology. *Food Funct*. 2020;11(7):6340–6351. doi:10.1039/D0FO01000F
20. Li J, Lu C, Jiang M, et al. Traditional Chinese medicine-based network pharmacology could lead to new multicompound drug discovery. *Evid Based Complement Alternat Med*. 2012;2012:149762. doi:10.1155/2012/149762
21. Jia ZL, Cen J, Wang JB, et al. Mechanism of isoniazid-induced hepatotoxicity in zebrafish larvae: activation of ROS-mediated ERS, apoptosis and the Nrf2 pathway. *Chemosphere*. 2019;227:541–550. doi:10.1016/j.chemosphere.2019.04.026
22. Li HY, Yang JB, Li WF, et al. In vivo hepatotoxicity screening of different extracts, components, and constituents of *Polygoni Multiflori* Thunb. in zebrafish (Danio rerio) larvae. *Biomed Pharmacother*. 2020;131:110524. doi:10.1016/j.biopha.2020.110524
23. Miyawaki I. Application of zebrafish to safety evaluation in drug discovery. *J Toxicol Pathol*. 2020;33(4):197–210. doi:10.1293/tox.2020-0021
24. Panzica-Kelly JM, Zhang CX, Danberry TL, et al. Morphological score assignment guidelines for the dechorionated zebrafish teratogenicity assay. *Birth Defects Res B Dev Reprod Toxicol*. 2010;89(5):382–395. doi:10.1002/bdrb.20260
25. Gfeller D, Grosdidier A, Wirth M, Daina A, Michielin O, Zoete V. SwissTargetPrediction: a web server for target prediction of bioactive small molecules. *Nucleic Acids Res*. 2014;42:W32–W38. doi:10.1093/nar/gku293
26. Keiser MJ, Roth BL, Armbruster BN, Ernsberger P, Irwin JJ, Shoichet BK. Relating protein pharmacology by ligand chemistry. *Nat Biotechnol*. 2007;25(2):197–206. doi:10.1038/nbt1284
27. Stelzer G, Rosen N, Plaschkes I, et al. The genecards suite: from gene data mining to disease genome sequence analyses. *Curr Protoc Bioinformatics*. 2016;54:1–30. doi:10.1002/cpbi.5
28. Shannon P, Markiel A, Ozier O, et al. Cytoscape: a software environment for integrated models of biomolecular interaction networks. *Genome Res*. 2003;13(11):2498–2504. doi:10.1101/gr.1239303
29. Dennis GJ, Sherman BT, Hosack DA, et al. DAVID: database for annotation, visualization, and integrated discovery. *Genome Biol*. 2003;4(5):P3. doi:10.1186/gb-2003-4-5-p3

30. Zaidun NH, Thent ZC, Latiff AA. Combating oxidative stress disorders with citrus flavonoid: naringenin. *Life Sci*. 2018;208:111–122. doi:10.1016/j.lfs.2018.07.017
31. Berman HM, Westbrook J, Feng Z, et al. The protein data bank. *Nucleic Acids Res*. 2000;28(1):235–242. doi:10.1093/nar/28.1.235
32. Yuan S, Chan H, Filipek S, Vogel H. PyMOL and inkscape bridge the data and the data visualization. *Structure*. 2016;24(12):2041–2042. doi:10.1016/j.str.2016.11.012
33. Trott O, Olson AJ. AutoDock Vina: improving the speed and accuracy of docking with a new scoring function, efficient optimization, and multithreading. *J Comput Chem*. 2010;31(2):455–461. doi:10.1002/jcc.21334
34. Hsin KY, Ghosh S, Kitano H. Combining machine learning systems and multiple docking simulation packages to improve docking prediction reliability for network pharmacology. *PLoS One*. 2013;8(12):e83922. doi:10.1371/journal.pone.0083922
35. Campbell I, Campbell H. Mechanisms of insulin resistance, mitochondrial dysfunction and the action of the ketogenic diet in bipolar disorder. Focus on the PI3K/AKT/HIF1-a pathway. *Med Hypotheses*. 2020;145:110299. doi:10.1016/j.mehy.2020.110299
36. Ren Z, Zhong H, Song C, et al. Insulin promotes mitochondrial respiration and survival through PI3K/AKT/GSK3 pathway in human embryonic stem cells. *Stem Cell Rep*. 2020;15(6):1362–1376. doi:10.1016/j.stemcr.2020.10.008
37. Okamoto A, Sumi C, Tanaka H, et al. HIF-1-mediated suppression of mitochondria electron transport chain function confers resistance to lidocaine-induced cell death. *Sci Rep*. 2017;7(1):3816. doi:10.1038/s41598-017-03980-7
38. Leadsham JE, Sanders G, Giannaki S, et al. Loss of cytochrome c oxidase promotes RAS-dependent ROS production from the ER resident NADPH oxidase, Yno1p, in yeast. *Cell Metab*. 2013;18(2):279–286. doi:10.1016/j.cmet.2013.07.005
39. Dejean L, Beauvoit B, Bunoust O, Guérin B, Rigoulet M. Activation of Ras cascade increases the mitochondrial enzyme content of respiratory competent yeast. *Biochem Biophys Res Commun*. 2002;293(5):1383–1388. doi:10.1016/S0006-291X(02)00391-1
40. Ye JH, Liu MH, Zhang XL, He JY. Chemical profiles and protective effect of Hedyotis diffusa Willd in lipopolysaccharide-induced renal inflammation mice. *Int J Mol Sci*. 2015;16(11):27252–27269. doi:10.3390/ijms161126021
41. Zhang Y, Yang X, Wang S, Song S, Yang X. Gentiopicroside prevents alcoholic liver damage by improving mitochondrial dysfunction in the rat model. *Phytother Res*. 2021;35(4):2230–2251. doi:10.1002/ptr.6981
42. Hua W, Zhang S, Lu Q, et al. Protective effects of n-Butanol extract and iridoid glycosides of Veronica ciliata Fisch. Against ANIT-induced cholestatic liver injury in mice. *J Ethnopharmacol*. 2021;266:113432. doi:10.1016/j.jep.2020.113432
43. Jayasuriya R, Dhamodharan U, Ali D, Ganesan K, Xu B, Ramkumar KM. Targeting Nrf2/Keap1 signaling pathway by bioactive natural agents: possible therapeutic strategy to combat liver disease. *Phytomedicine*. 2021;92:153755. doi:10.1016/j.phymed.2021.153755
44. Wang K, Deng Y, Zhang J, et al. Toxicity of thioacetamide and protective effects of quercetin in zebrafish (Danio rerio) larvae. *Environ Toxicol*. 2021;36(10):2062–2072. doi:10.1002/tox.23323
45. Franke TF. PI3K/Akt: getting it right matters. *Oncogene*. 2008;27(50):6473–6488. doi:10.1038/onc.2008.313
46. Luo J, Manning BD, Cantley LC. Targeting the PI3K-Akt pathway in human cancer: rationale and promise. *Cancer Cell*. 2003;4(4):257–262. doi:10.1016/S1535-6108(03)00248-4
47. Song G, Ouyang G, Bao S. The activation of Akt/PKB signaling pathway and cell survival. *J Cell Mol Med*. 2005;9(1):59–71. doi:10.1111/j.1582-4934.2005.tb00337.x